Analyst

ROYAL SOCIETY OF CHEMISTRY

PAPER

View Article Online
View Journal | View Issue

Cite this: *Analyst*, 2026, **151**, 466

Identification of organochlorides in distilled fractions of plastic pyrolysis oil using GC × GC coupled with high-resolution time-of-flight mass spectrometry (GC × GC-HR-TOFMS) and GC coupled with a halogen selective detector (GC-XSD)

Bruno da Costa Magalhães, Pascal Pijcke, Niels Verhoosel, Philip Janssen, Cesare Benedetti, Matthijs Ruitenbeek, Georgios Bellos and Melissa N. Dunkle *

Received 8th August 2025,
Accepted 13th November 2025

DOI: 10.1039/d5an00852b

rsc.li/analyst

To support the transition toward a more circular economy, various technologies have been explored to convert plastic waste into valuable materials. Among these is pyrolysis, a thermochemical process that produces gas, solid, and liquid products, where the latter is known as plastic pyrolysis oil (PPO). These oils typically contain hydrocarbons and impurities such as oxygenates, nitrogenates, and organochlorides, depending on the composition of the plastic feedstock and process conditions. Since these contaminants must be removed before PPOs can be used in industrial steam crackers, their speciation is essential to define appropriate upgrading strategies. In this context, this study evaluates a gas chromatograph coupled with a halogen selective detector (GC-XSD) system, in combination with a comprehensive gas chromatograph system coupled with high resolution time-of-flight mass spectrometry (GC × GC-HR-TOFMS), for the identification of organochlorides in hydrocarbon matrices. Initially, the selectivity of the XSD, reactor temperature, and response to Cl standards were assessed. The method was then applied to the distilled fractions of a PPO. Using GC × GC-HR-TOFMS, several organochlorides were identified, including 1-chlorobutane, which was found at the highest concentration in the first distilled fraction (50–100 °C), and 3-(chloromethyl)heptane and 1,3-dichlorobezene, which were eluted primarily in the third fraction (150–200 °C). Other compounds, such as 1,2-dichloroethane, chlorobenzene, and 2-chloroethyl benzoate, were also detected at lower concentrations. The GC-XSD was proved to exhibit robust and selective capability for organochloride speciation in PPOs and could be potentially implemented in quality control and routine laboratories. When combined with hyphenated techniques such as GC × GC-HR-TOFMS, GC-XSD also facilitates the identification of unknown organochlorides.

1. Introduction

Due to their unique and versatile properties, plastics are widely used in various applications, including packaging, automotive and construction parts, and healthcare. However, this widespread use results in the generation of substantial plastic waste, much of which ends up in landfills or is disposed of *via* incineration.[1] To move toward a more circular economy, where plastic waste is reused to produce new materials, plastic recycling is a preferred pathway to avoid waste and retain carbon in the materials loop.

Two primary recycling approaches are employed: mechanical recycling and chemical recycling. While mechanical recycling is currently more established, chemical recycling offers the advantage of processing materials that are difficult to recycle mechanically.[2] Technologies used in chemical recycling include depolymerization, pyrolysis, and gasification. Among these, pyrolysis is a thermochemical process that is currently implemented by several companies. It produces three main products: a gas phase, a solid residue known as char, and a liquid fraction referred to as plastic pyrolysis oil (PPO).[3]

PPOs are known to contain a complex mixture of hydrocarbons, and various impurities, such as oxygenates, nitrogenates, and organochlorides.[4–9] These impurities hinder the direct use of PPOs as a feedstock to steam crackers.[10–13]

Dow Benelux BV, Herbert H. Dowweg 5, 4542 NM Hoek, The Netherlands.
E-mail: mndunkle@dow.com

Therefore, an upgrading step, such as hydrotreatment (HDT), is required to convert PPO into feedstock suitable for producing virgin materials. HDT is a well-established technology traditionally used to improve the quality of fossil-derived oils, such as reducing sulfur content in diesel to meet regulatory standards. While HDT is effective in saturating olefins and aromatics and removing nitrogenates and oxygenates, the presence of organochlorides in PPOs presents a significant challenge.

Organochlorides can originate from polymers with chlorine in their backbone, such as polyvinyl chloride (PVC) and polyvinylidene chloride (PVDC), as well as from additives and impurities from cross-contamination in waste handling. The amount of chlorine in PPO can be up to hundreds of ppm.[14,15] In contrast, many refineries impose a maximum chlorine limit of 1 ppmw (mg kg^{-1}) to prevent downstream issues.[16]

The hydroprocessing of oils with high chlorine content can lead to the formation of hydrogen chloride (HCl), a highly corrosive compound that necessitates the use of more expensive, corrosion-resistant materials. Additionally, HCl can react with ammonia (NH_3), a by-product of hydrodenitrogenation, to form ammonium chloride salts. These salts may precipitate in pipelines or dissolve in process water, resulting in sour water.[17,18] Furthermore, the presence of HCl can accelerate catalyst deactivation, as reported in previous studies involving PPO hydroprocessing.[19,20]

In this context, the speciation of organochlorides in plastic pyrolysis oils (PPOs) becomes critically important. Understanding the specific types of organochlorides present can provide valuable insights into their formation mechanisms during the pyrolysis process and create strategies for their effective removal prior to upgrading or utilizing PPOs. Recently, Souchon *et al.*[21] described the hyphenation of gas chromatography with inductively coupled plasma tandem mass spectrometry (GC-ICP-MS/MS) for the analysis of organochlorides in hydrocarbon samples, including naphtha fractions derived from PPOs. This system demonstrated linearity and equimolar response for the quantification of chlorine-containing compounds, as previously shown by Nelson *et al.*[22] in other matrices. Additionally, in a previous publication, we presented a methodology for organochloride identification in PPOs using scripting expressions to filter data obtained from comprehensive two-dimensional gas chromatography coupled with high-resolution time-of-flight mass spectrometry (GC × GC-HR-TOFMS).[23] While these approaches proved to be highly effective and informative, such hyphenated techniques are not suitable for routine use in quality control laboratories due to their complexity. As an alternative or complementary approach, gas chromatography (GC) coupled with a selective detector could be employed. This setup offers a more practical and accessible solution for routine monitoring while still enabling targeted detection of specific compounds. Such an approach has been used for the speciation of organochlorides in both fossil- and bio-based oils. Selective detectors that can be considered include the electron capture detector (ECD),[17,18,24] the atomic emission detector (AED), the electrolytic conductivity detector (ELCD),[25] and the halogen-selective detector (XSD).[26,27]

Liu *et al.*[24] evaluated the use of GC coupled with an electron capture detector (ECD) in combination with MS for the characterization of chlorinated and oxygenated compounds in PPOs derived from paper mill waste. While this method enabled the identification of several organochlorides, such as 1,2-dichloroethane, 1,2-dichlorobenzene, and 2,2-dichloropropane, these compounds accounted for only 14% of the total chlorine content. Moreover, the study reported uncertainty regarding whether some oxygenates, nitrogenates, and polyaromatic hydrocarbons could also produce ECD signals, potentially leading to false positives.

In a more recent study, Giri *et al.*[27] developed a GC-XSD method and applied it to 51 oil samples, including PPOs. This approach enabled the detection of 59 organochloride compounds, supported by GC × GC-TOFMS analysis, analytical standards, and retention index data. This comprehensive study highlights the XSD as a promising tool for the speciation of organochlorides in PPOs. This detector had also been used previously by Zhuang *et al.*[26,28] for the analysis of chlorinated fatty acids in different matrices. Although they reported that the XSD was not superior to other GC detectors in terms of signal-to-noise ratio, it demonstrated high selectivity, low detection limits, and was noted for its ease of operation and maintenance. Additionally, it is worth mentioning that, unlike the ECD, the XSD does not require a radioactive source.

Therefore, this study aims to apply and evaluate a GC-XSD method, in combination with GC × GC-HR-TOFMS, for the identification of organochlorides in the distilled fractions of plastic pyrolysis oil. Distillation fractions were utilized to reduce the complexity of the crude PPO prior to analysis and to enable a more detailed identification of which species are present in the lighter and heavier fractions. In addition, the influence of key detector parameters, such as operating temperature, response factors for various organochlorides, and selectivity in the presence of hydrocarbon matrices, is also discussed.

2. Materials and methods

a. Reagents

A light and middle distillate, a PPO sample and its distilled fractions, and solutions containing various chlorine standards in toluene (VWR, ≥99.9%) were prepared. The chlorine standards used were 1,2,3-trichlorobenzene (Sigma Aldrich, ≥99%), 1,2,4-trichlorobenzene (Sigma Aldrich, ≥99%), 1,2-dichlorobenzene (Sigma Aldrich, 99%), 1,2-dichloroethane (Sigma Aldrich, ≥99%), 1,3,5-trichlorobenzene (Sigma Aldrich, ≥99%), 1,3-dichlorobenzene (Sigma Aldrich, 98%), 1,4-dichlorobenzene (Sigma Aldrich, ≥99%), 1,5-dichloropentane (TCI Europe N.V., >95%), 1-chloro-2-propanol (Sigma Aldrich, 70%), 1-chloro-3-methylbutane (TCI Europe N.V., >98%), 1-chlorobutane (TCI Europe N.V., >98%), 1-chlorooctane (Sigma Aldrich, 99%), 1-chloropentane (TCI Europe N.V., >99%), 2,4,6-trichloroanisole (Sigma Aldrich, 99%), 2-chloro-2-methylbutane (TCI Europe N.V., >97%), 2-chloro-2-propen-1-ol (Sigma Aldrich,

90%), 2-chlorobenzonitrile (TCI Europe N.V., >98%), 2-chloroethyl benzoate (TCI Europe N.V., >99%), 2-chloromethyl-1,3-dioxolane (Sigma Aldrich, 97%), 2-chlorophenol (Sigma Aldrich, ≥99%), 3,4-dichlorobenzamide (TCI Europe N.V., >98%), 3,5-dichlorophenol (Sigma Aldrich, 97%), 3-(chloromethyl)heptane (Supelco, 97%), 3-chloro-1-butene (TCI Europe N.V., >62%), 3-chlorobenzonitrile (TCI Europe N.V., >98%), 3-chlorophenol (Sigma Aldrich, ≥98%), 4-chloro-1-butene (TCI Europe N.V., >98%), 4-chloroanisole (Sigma Aldrich, 99%), 4-chlorobenzonitrile (TCI Europe N.V., >98%), 4-chlorophenol (Sigma Aldrich, ≥99%), 5-chlorobenzotriazole (Sigma Aldrich, 99%), chlorobenzene (Sigma Aldrich, 98%), chloroform (VWR, 99.8%), dichloromethane (VWR, 100%), and *trans*-1,2-dichlorotethylene (Fluka, 97.0%).

b. Distillation of crude plastic pyrolysis oil

A Quickdist 500CC unit was used to distil approximately 1 liter of plastic pyrolysis oil into seven fractions, each corresponding to a specific boiling point range: initial boiling point (IBP)–100 °C, 100–150 °C, 150–200 °C, 200–250 °C, 250–300 °C, 300–350 °C, and >350 °C. The initial distillation pressure was set at 763 Torr and was gradually reduced to 1 Torr for the heavier fractions. A device was used to convert the measured boiling point into an equivalent normal boiling point. The distillation was carried out using a 2000 mL round-bottom flask, placed on a magnetic stirring unit and heated with a high-power mantle heater capable of reaching 550 °C. One neck of the flask was connected to a quench cooler, while the other was attached to a packed separation column (580 mm of Sulzer EX packing), which was thermally insulated with a vacuum mantle, silver coating, and mantle heater. At the top of the column, a condenser was installed, with its temperature controlled by a refrigerated circulator using a glycol cooling fluid (Thermal G). A vacuum line was connected to the top of the condenser to maintain reduced pressure during the distillation. The condenser was connected to an intermediate receiver *via* a temperature-controlled line. A reflux valve regulated the flow between the condenser and the receiver, typically operating at a 4 : 40 ratio, except during the distillation of the 200–250 °C cut, where a 4 : 20 ratio was used to account for the boiling behavior of naphthalene. The intermediate receiver transferred its contents to a final receiver using nitrogen pressure, either when the receiver was full or when the temperature sensor of the condenser reached the target value. To prevent overpressure or overfilling, a secondary needle provided a pressure relief path to a washing flask. Additional information regarding the distillation experiment and the composition of the resulting fractions has been reported elsewhere.[29]

c. Comprehensive gas chromatography coupled with high-resolution time-of-flight mass spectrometry (GC × GC-HR-TOFMS)

A gas chromatograph (Agilent Technologies 7890B) equipped with a cryogenic modulator was coupled to a high-resolution time-of-flight mass spectrometer (HR-TOFMS, LECO Instruments GmbH, Mönchengladbach, Germany) for analysis. Sample injection was performed with a volume of 1 μL in a split/splitless inlet using a 100 : 1 split ratio at 280 °C. The chromatographic separation employed a reverse-phase setup, consisting of a VF-200ms column (35% trifluoropropyl methyl polysiloxane/65% dimethylpolysiloxane: 30 m × 0.25 mm × 0.25 μm) as the first dimension and a DB-1ms column (100% dimethylpolysiloxane: 0.55 m × 0.10 mm × 0.4 μm) as the second dimension. Helium was used as the carrier gas at a constant flow rate of 1.0 mL min^{-1}. The modulation time was set to 5 seconds, with a hot pulse duration of 1.5 seconds. The oven temperature program began at 30 °C (held for 2 minutes), followed by a ramp of 5 °C min^{-1} to 280 °C, where it was held for 5 minutes. The transfer line to the detector was maintained at 280 °C, and the total run time was 50 minutes. Perfluorotributylamine (PFTBA) was injected during the GC run to serve as a mass calibrant. Mass correction was applied during data processing using the calibrant signal. The HR-TOFMS was operated in positive ion mode with electron impact ionization (EI) at 70 eV. The ion source temperature was set to 250 °C, and the scan rate was 100 spectra per second. Data from the HR-TOFMS were processed using ChromaTOF software (v.90.62.0.49093) with the integrated spectral analysis tools. Additional details on the chromatographic method, and the data filtering approach applied to HR-TOFMS results are provided in our previous study.[23]

d. Gas chromatography coupled with a halogen selective detector and a flame ionization detector (GC-XSD/FID)

A gas chromatograph (Agilent Technologies 7890B) with a HP-PONA (100% dimethylpolysiloxane: 50 m × 0.200 mm × 0.5 μm) or a VF-200ms (35% trifluoropropyl methyl polysiloxane/65% dimethylpolysiloxane: 30 m × 0.25 mm × 1 μm) column and a splitter was coupled to a halogen selective detector (XSD) (Da Vinci Laboratory Solutions, The Netherlands) and a flame ionization detector (FID). Both signals were acquired simultaneously. 0.2 μL was injected into a split/splitless liner at 250 °C with a split ratio of 100 : 1. Helium was used as the carrier gas at a constant flow rate of 1.5 mL min^{-1}. The oven was kept at 40 °C for 2 min and then heated up until 280 °C (10 °C min^{-1}) and kept at this temperature for an additional 4 min. The XSD was kept at 800–1100 °C with an air flow of approximately 20 mL min^{-1}. The FID was kept at 300 °C. The system was controlled *via* the OpenLab CDS Acquisition software (2.5.0.842), and the Agilent OpenLab Data Analysis package (2.205.0.1344) was used to treat the data.

e. Combustion ion-chromatography (C-IC)

Total chlorine content was measured *via* combustion ion-chromatography (C-IC) using a Trace Elemental (Delft, the Netherlands) Xprep C-IC system, consisting of an Archie autosampler, an Xplorer combustion unit, an Xprep absorption unit, and a Metrohm 930 IC system. The calibration of the C-IC method was performed directly using the boat with the autosampler. Using Trace Elemental Instruments Analytical Software, the first heater zone was heated to 750 °C and the

second zone to 1000 °C. Then, using Magicnet 4.0 software, 30 μL of sample was injected with an autosampler into the boat inlet system. With pyrohydrolytic combustion in an oxygen-rich environment and at high temperatures, the sample was completely oxidized. Halogens present in the sample were converted to H–X and X_2. After combustion, the output gas stream containing the analytes was transferred to an absorber unit and trapped in the absorber medium. The absorber unit handled the rinsing and dosing of required absorber medium, including hydrogen peroxide solution (H_2O_2). This process converts the H–X and X_2 to F^-, Cl^-, and Br^-. After sample preparation, an aliquot of the absorber solution containing the analytes was injected into an IC instrument by a sample injection valve. The halide anions were separated on the separator column of the IC. The conductivity of the eluent was reduced with an anion suppression device before the eluent reached the electrical conductivity detector of the ion chromatograph, where the anions of interest were analyzed. Results were quantified according to a calibration curve. The total analysis time for each sample was 20 min.

3. Results and discussion

a. Halogen selective detector evaluation

i. Selectivity: matrix effect. As is well known, PPOs derived from polyolefin-rich waste contain a wide range of compounds, including olefins and aromatics at weight-percentage levels, while impurities such as oxygenates, nitrogenates, and organochlorides are typically present at ppm levels.[30] Even with advanced techniques like comprehensive two-dimensional gas chromatography, identifying these trace-level species remains challenging. The difficulty increases when using one-dimensional systems, where coelution is more common. In this context, the following section presents a methodology developed to facilitate the identification of organochlorides in PPOs, leveraging the selectivity of the XSD detector. To evaluate the selectivity of the XSD detector toward halogen-containing compounds, specifically organochlorides, two different hydrocarbon matrices, a light and a middle distillate, were spiked with various Cl standards. The chlorine concentration ranged from 15 to 100 mg L^{-1}. Fig. 1 presents the chromatograms obtained for both matrices using two different detectors: an FID and an XSD. Both signals were acquired simultaneously. The retention times of the different Cl standards are reported in Table S1. On the one hand, although hydrocarbons are present at weight-percentage levels in the samples, only minor interferences were observed in the XSD chromatogram. On the other hand, organochlorides were clearly detected by the XSD, even at low concentrations and in cases of coelution with other hydrocarbons. This highlights the high selectivity of the XSD detector, which is particularly valuable when analyzing complex feedstocks.

ii. Organochloride identification. Two different columns were employed for the GC-XSD evaluation: HP-PONA (100% dimethylpolysiloxane) and VF-200ms (35% trifluoropropyl methyl polysiloxane/65% dimethylpolysiloxane). While the HP-PONA column offers the advantage of extensive retention index data, our previous work[23] demonstrated that, in a comprehensive GC × GC system, a column set composed of VF-200ms (first dimension) and DB-1 (second dimension) enabled effective separation of most organochlorides from the hydrocarbon matrix.

Based on this, several chlorine standards were analyzed using both: the previously mentioned GC × GC-HR-TOFMS system and the GC-XSD system equipped with a VF-200ms column. This approach allowed for the correlation of retention times between the two systems, as illustrated in Fig. 2. The retention time of the different Cl compounds is reported in Table S2. Due to differences in the temperature programs of the two systems, two distinct linear trends were observed: one from the beginning of the run up to approximately 7 minutes, and another extending to the end of the run.

This strategy was also reported by Giri *et al.*,[27] who evaluated a GC-XSD method using a DB-1 column in both the GC-XSD and as the first dimension in the GC × GC-TOFMS setup. Additionally, our group has applied this methodology to speciate other contaminants, such as nitrogen-containing compounds. For example, a GC method coupled with a nitrogen chemiluminescence detector (NCD) was used similarly to the GC-XSD, improving the identification of nitrogenates[29]. This approach becomes particularly powerful when the GC × GC system is coupled with HR-TOFMS, which provides high-confidence molecular identification and enables the use of advanced data processing techniques, such as mass defect plots. As shown in our previous work,[23] this feature is especially useful for organochlorides, which exhibit distinct mass defects compared to hydrocarbons and other species, particularly when using a Cl–H mass defect scale.

Therefore, the correlation between a GC-XSD method and GC × GC-HR-TOFMS can be highly effective for the identification of unknown compounds. Once new species are identified using GC × GC-HR-TOFMS, they can be added to the GC-XSD method, allowing retention time to serve as a reliable indicator of their presence in future analyses. In the following section, the effect of the XSD reactor temperature, a critical parameter that influences detector performance, is discussed.

iii. Impact of XSD reactor temperature. One of the solutions previously mentioned, containing several Cl standards, with chlorine concentrations ranging from 15 to 100 mg L^{-1} spiked into the light distillate, was analyzed using different XSD reactor temperatures. The detector allows manual selection of four reactor temperatures: 800 °C, 900 °C, 1000 °C, and 1100 °C. GC parameters such as injection volume and split ratio were kept constant across all four runs.

As is well known, the XSD operates in an oxidative mode. During the analysis, the effluent from the GC column is pyrolyzed, converting halogen-containing compounds into their oxidation products and free halogen atoms. These atoms are adsorbed onto and react with an alkali-sensitized cathodic bead, resulting in increased thermionic emission. This emission, composed of free electrons and halogen ions, is

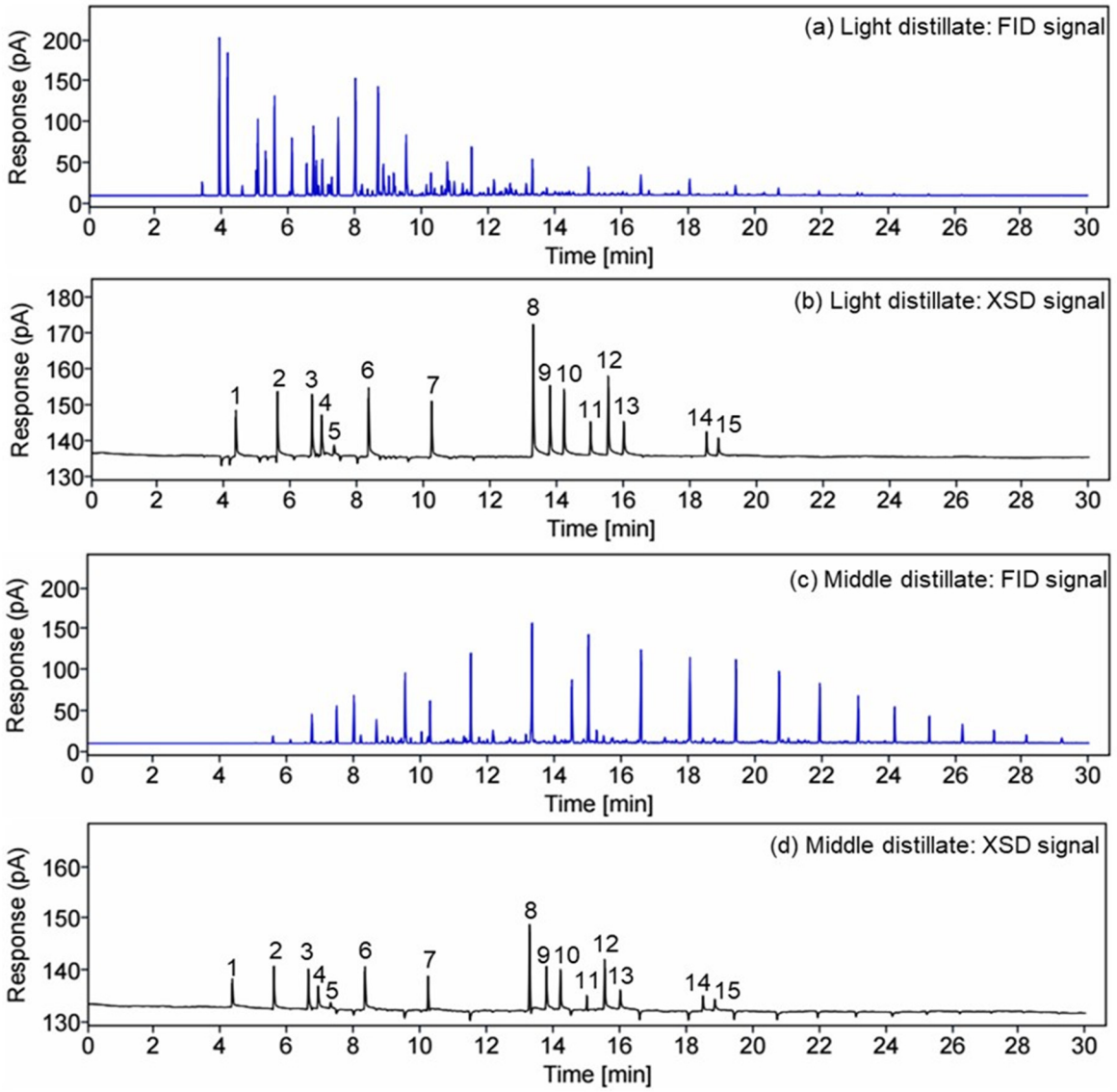

Fig. 1 Cl standards spiked in hydrocarbon matrices with a chlorine concentration ranging from 15 to 100 mg L^{-1}: (a) light distillate: FID signal; (b) light distillate: XSD signal; (c) middle distillate: FID signal; (d) middle distillate: XSD signal. The Cl standards are: (1) dichloromethane; (2) chloroform; (3) 2-chloro-2-methylbutane; (4) 1-chloro-2-propanol; (5) impurity: 2-chloro-1-propanol; (6) 1-chloropentane; (7) chlorobenzene; (8) 1,3-dichlorobenzene; (9) 1,2-dichlorobenzene; (10) 1-chlorooctane; (11) 1,3,5-trichlorobenzene; (12) 3-chlorobenzonitrile; (13) 3-chlorophenol; (14) 2,4,6-trichloroanisole; (15) 3,5-dichlorophenol.

measured by an electrometer and converted into an output signal.

The peak areas obtained for the various Cl standards at each reactor temperature are presented in Table 1. Values in parentheses indicate the percentage increase in area at temperature "T + 100 °C" compared to the area obtained at temperature "T" for the same compound. For example, an increase in area of 302.7% was noticed for dichloromethane when the reactor temperature was increased from 800 °C to 900 °C.

Increasing the reactor temperature significantly enhanced the detector response for all Cl standards, while no significant difference was noticed in the instrument noise. An increase of over 200% in peak area was observed for nearly all compounds when the temperature was raised from 800 °C to 900 °C, and again from 900 °C to 1000 °C. However, the increase was less pronounced between 1000 °C and 1100 °C, suggesting that 1000 °C may be suitable for most applications, while the highest temperature can be used when even lower detection limits are needed.

According to Zhuang *et al.*,[28] who thoroughly investigated the influence of operating conditions on chromatographic and XSD responses, the improved sensitivity at higher temperatures is likely due to a shift in equilibrium toward the formation of chlorine atoms. In other words, higher temperatures generate a greater concentration of chlorine atoms, leading to a more intense detector response.

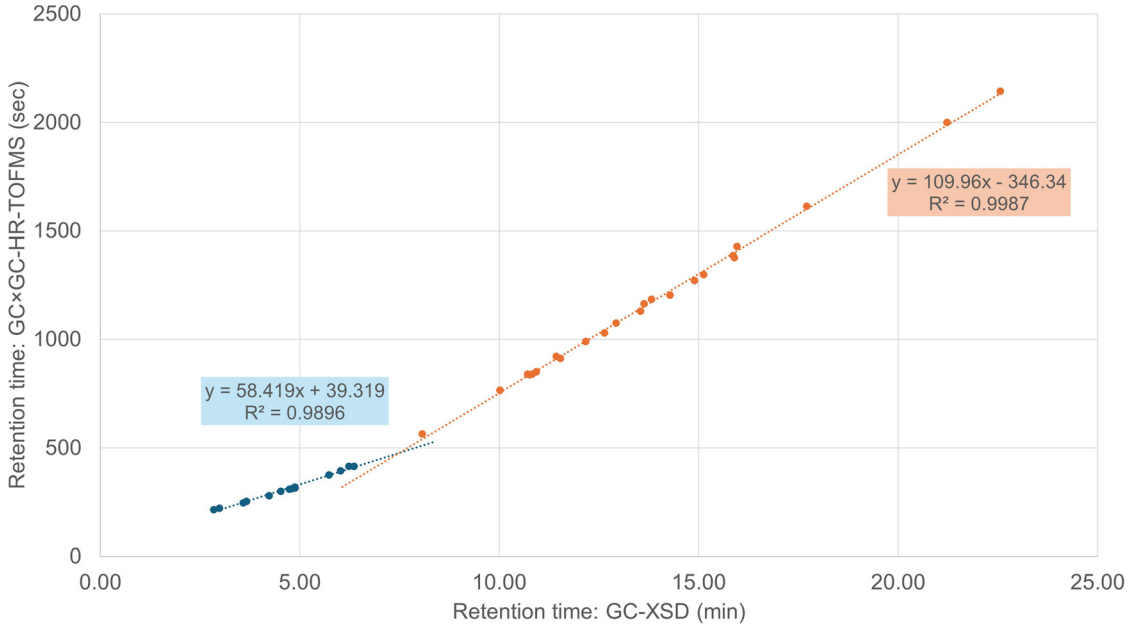

Fig. 2 Retention time correlation between GC × GC-HR-TOFMS and GC-XSD.

Table 1 Impact of XSD reactor temperature on the peak area of Cl standards spiked in light distillate with a chlorine concentration ranging from 15 to 100 mg L^{-1}

	XSD reactor temperature			
Cl standard	800 °C	900 °C	1000 °C	1100 °C
Dichloromethane	1.7	7.0 (303%)	25.8 (266%)	53.9 (109%)
Chloroform	3.6	11.8 (230%)	38.4 (227%)	72.3 (88%)
2-Chloro-2-methylbutane	3.1	12.0 (286%)	36.2 (203%)	65.6 (81%)
1-Chloro-2-propanol	2.3	8.9 (281%)	25.9 (192%)	52.2 (102%)
1-Chloropentane	3.5	12.8 (265%)	63.8 (399%)	69.5 (9%)
Chlorobenzene	2.7	10.2 (271%)	31.1 (206%)	57.5 (85%)
1,3-Dichlorobenzene	6.5	23.2 (254%)	77.7 (235%)	152.2 (96%)
1,2-Dichlorobenzene	3.2	11.9 (277%)	41.5 (249%)	79.3 (91%)
1-Chlorooctane	3.1	11.9 (281%)	35.9 (202%)	70.0 (95%)
1,3,5-Trichlorobenzene	1.7	6.3 (275%)	19.6 (213%)	37.9 (93%)
3-Chlorobenzonitrile	3.6	13.0 (263%)	46.1 (256%)	84.9 (84%)
3-Chlorophenol	1.7	6.7 (302%)	22.4 (235%)	40.3 (80%)
2,4,6-Trichloroanisole	1.3	4.2 (234%)	13.0 (210%)	22.6 (74%)
3,5-Dichlorophenol	1.0	3.0 (220%)	11.2 (269%)	21.3 (90%)

The values within parentheses refer to the relative increase in the peak area obtained at reactor temperature "T + 100 °C" compared to the obtained area at temperature "T" for the same Cl standard.

However, as mentioned by the same authors, operating at elevated temperatures may accelerate the depletion of the potassium reservoir in the XSD reactor, reducing the probe's lifetime and requiring more frequent replacement.

Therefore, the XSD reactor temperature can be selected based on the total chlorine content of the sample and the level of speciation required. Although this study did not attempt to evaluate the effect of chromatographic parameters, factors such as injection volume and split ratio can also be optimized depending on the sample matrix and chlorine content.

iv. Response factor of XSD for different Cl standards. The response factors of the XSD toward various Cl standards, including linear, aromatic, oxygen-, and nitrogen-containing compounds, were evaluated by establishing calibration curves using chlorine concentrations ranging from 0 to 25 mg L^{-1} in toluene. The response factors were defined as the slopes of the respective calibration curves, calculated from nine calibration points. Fig. 3 presents the linear correlations obtained for the different standards. A more comprehensive list is provided in the SI (Table S3), which includes response factors calculated from single-point measurements. In these cases, the response factor was obtained by dividing the peak area by the corresponding chloride concentration.

A high correlation ($R^2 \geq 0.99$) was observed for all standards within the tested concentration range, indicating that the detector response is proportional to the amount of chlorine

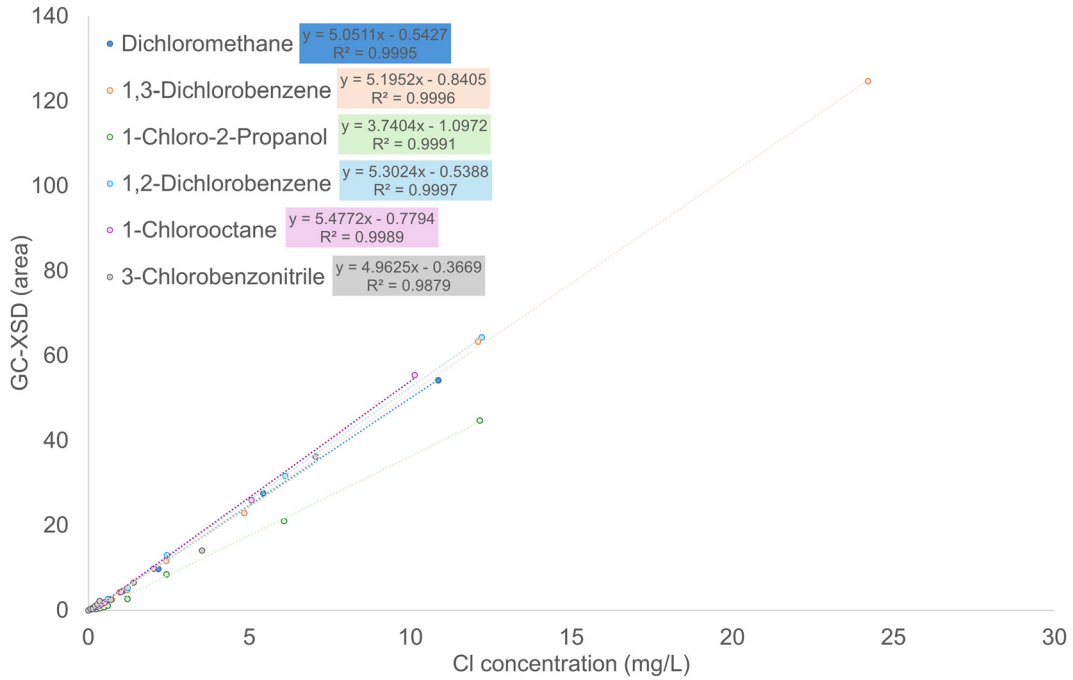

Fig. 3 Calibration curves for Cl standards with different chemical functionalities obtained using the XSD.

present in each blend. Although some compounds exhibited similar response factors, as also shown in Table S3, deviations of up to 32% were observed with respect to the response factor average, for example, in the case of 1-chloro-2-propanol. This suggests that certain compounds, depending on their functional groups, are more challenging to quantify, likely due to variations in detector response as well as differences in chromatographic peak shape and resolution.

These results highlight the importance of preparing calibration curves with a proper standard to ensure accurate quantification. In other words, the XSD does not exhibit an equimolar response at the chlorine concentration evaluated, unlike sulfur and nitrogen chemiluminescence detectors (SCD and NCD, respectively). This limitation may require extensive laboratory work to prepare appropriate standards. Furthermore, given that the composition of PPOs can vary significantly depending on the feedstock and pyrolysis conditions, suitable standards may not always be commercially available. In this context, the use of alternative detectors or systems, such as the atomic emission detector (AED) or inductively coupled plasma tandem mass spectrometry (ICP-MS/MS), which is expected to provide an equimolar response to chlorine, may offer advantages and could be beneficial to evaluate further.

Therefore, as demonstrated in this section, the XSD method proved to be selective for organochlorides in hydrocarbon matrices such as light and middle distillates. Although fluorine- and bromine-containing species are also known to produce signals in XSD chromatograms, the detector exhibits lower sensitivity to these elements compared to chlorine, according to the manufacturer.

Moreover, the combined use of GC-XSD and GC × GC-HR-TOFMS has proven valuable for the identification of unknown compounds. This integrated approach enhances the ability to detect and characterize trace-level organochlorides in complex matrices. Additionally, a reactor temperature of at least 1000 °C was found to be suitable for the purposes of this study, which aims to speciate organochlorides present at ppm levels. While the detector did not exhibit an equimolar response across all compounds, a linear correlation was observed within the concentration range of 0 to 25 mg L^{-1}.

These findings confirm that the XSD is a powerful and selective detector for the speciation of organochlorides in hydrocarbon matrices. In the next section, the GC-XSD method, combined with other analytical techniques, is applied to the distilled fractions of a plastic waste-derived pyrolysis oil.

b. Application to the distilled fractions of plastic pyrolysis oil

A crude PPO sample was distilled into several fractions with steps of 50 °C. The first three fractions fall within the boiling range of naphtha and natural gas condensate (<200 °C), while the remaining fractions correspond more closely to the diesel range (200–350 °C). The total chlorine content, measured by combustion ion chromatography, is presented in Fig. 4 for each fraction. The total chlorine content in the undistilled PPO was 67 mg L^{-1}, while the cumulative chlorine content across all distilled fractions was 64 mg L^{-1}. It is worth noting that a residual fraction with a boiling point above 350 °C was also obtained. This fraction had a waxy consistency and was not further analyzed, as it represented only 2.6 wt% of the total PPO. Consequently, this fraction is not discussed in this study. Additionally, minor losses were also observed during the distillation experiment.

The distribution of organochlorides varied significantly with boiling point. While the first and third fractions exhibited

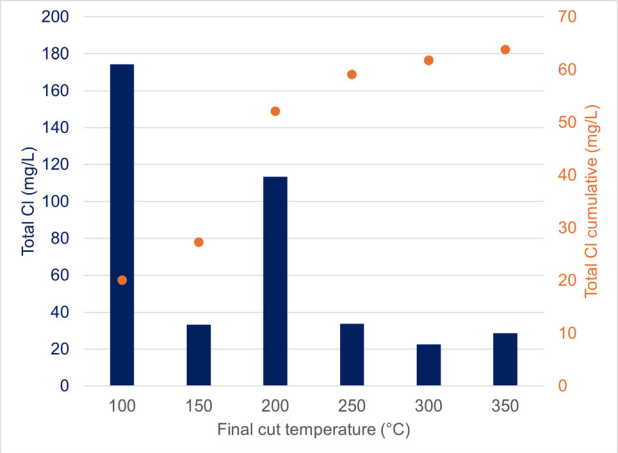

Fig. 4 Chlorine content (mg L^{-1}), shown in blue, of the distilled fractions of plastic pyrolysis oil obtained from combustion ion chromatography, and cumulative chlorine content (mg L^{-1}), shown in orange, based on the chlorine content and mass of each fraction collected during distillation.

chlorine concentrations exceeding 100 mg L^{-1}, all other fractions contained Cl concentrations of less than 30 mg L^{-1}. The amount of distilled material recovered from the first fraction accounted for 11.5 wt% of the PPO, while the subsequent fractions accounted for 21.7 wt%, 21.9 wt%, 20.8 wt%, 11.8 wt%, and 7.1 wt%, respectively. The remaining material was retained as residue, as previously discussed.

Notably, the first and third fractions alone accounted for 67% of the total chlorine content in the crude PPO. These two fractions would typically be classified within the naphtha boiling point range. In contrast, the lower chlorine concentrations in the other fractions contributed to a PPO with relatively reduced overall chlorine content.

These findings underscore the importance of this study, particularly considering that dilution is a key strategy for enabling the use of PPO in existing industrial facilities. In scenarios where only the naphtha-range fractions are considered as steam cracker feedstock, higher dilution ratios would be required to meet chlorine specifications.

Moreover, the undistilled PPO and its distilled fractions were analyzed using the GC-XSD method. The chromatograms obtained from the distilled fractions are presented in Fig. 5, highlighting several identified organochlorides. These species were characterized by comparing their retention time with Cl standards and by using the retention time approach, described in a previous section, which correlated the GC-XSD with the GC × GC-HR-TOFMS system. A few GC × GC chromatograms of the undistilled oil and distilled fractions were provided in our previous publication.[29] This strategy involved two main steps: first, scripting expressions were applied to filter the HR-TOFMS data. Then, the filtered components were tentatively identified based on matches with the mass spectral library, NIST 2020, as discussed in our previous study.[23] Major peaks observed in the GC-XSD chromatograms were also cross-checked to ensure they were captured by the scripting approach and identified.

Notably, 1-chlorobutane was detected as the most prominent Cl compound in the first fraction, followed by 4-chloro-1-butene, and 1,2-dichloroethane. In the second fraction, chlorobenzene, ethanol, 2-chloro-, acetate, and 1,4-dichlorobutane were identified, while the third fraction contained mostly 3-(chloromethyl)heptane and 1,3-dichlorobenzene. The fourth fraction revealed the presence of trichlorobenzenes and 2-chloroethyl benzoate. Several extracted ion chromatograms (XIC) obtained with the GC × GC-HR-TOFMS system are presented in the SI, Fig. S1–S9, confirming the presence of organochlorides across the different distilled fractions.

The GC-XSD method proved highly effective in highlighting components present at higher concentrations, while filtering HR-TOFMS data provided a rapid overview of all the organochlorides present in the sample. Additionally, the analysis of the distilled fractions also revealed minor peaks that would have been difficult to detect in the undistilled sample due to their low concentrations, highlighting the benefit of fractionation for improved identification.

Chromatograms of the undistilled PPO obtained using both FID and XSD detectors are shown in Fig. 6(a) and (b), respectively. The FID signal reveals the presence of numerous hydrocarbons, present at weight-percentage levels. In addition, various impurities such as oxygenates and nitrogen-containing compounds were also present. In contrast, the GC-XSD chromatogram clearly showed several organochlorides, even at low ppm levels, while no false positives being found, confirming the selectivity of this detector in such a complex matrix.

In the GC-XSD chromatogram, three prominent peaks at relatively higher concentrations were clearly visible. The first peak (labelled as peak 2) eluted primarily in the first fraction, while the other two (peaks 7 and 8) were mainly found in the third fraction, in agreement with the total chlorine content previously measured in these fractions. Additionally, several other peaks were observed with (much) lower intensities, particularly in the higher boiling point fractions, which also hinder the identification of these organochlorides.

The identification of various organochlorides in PPOs can provide valuable insights into their formation mechanisms during the pyrolysis process. For example, as reported by Giri *et al.*,[27] 3-(chloromethyl)heptane may be generated through an SN2 mechanism, where a chlorine ion serves as the nucleophile and attacks bis(2-ethylhexyl)phthalate (DEHP), a plasticizer frequently used in PVC formulations, as shown in Fig. 7. In this reaction, the chlorine ion replaces the ester-linked group, with the phthalate ester acting as the leaving group. In addition to 3-(chloromethyl)heptane, Giri *et al.*[27] also identified several other organochlorides, including 2-chloroethanol, ethylchloride, 2-chloroethyl benzoate, ethanol, 2-chloroacetate, and 1,2-dichloroethane, as among the most frequently observed organochlorides across multiple oils, including PPOs. As previously discussed, a few compounds were also detected in the present study, except for 3-(chloromethyl) heptane, at lower concentrations.

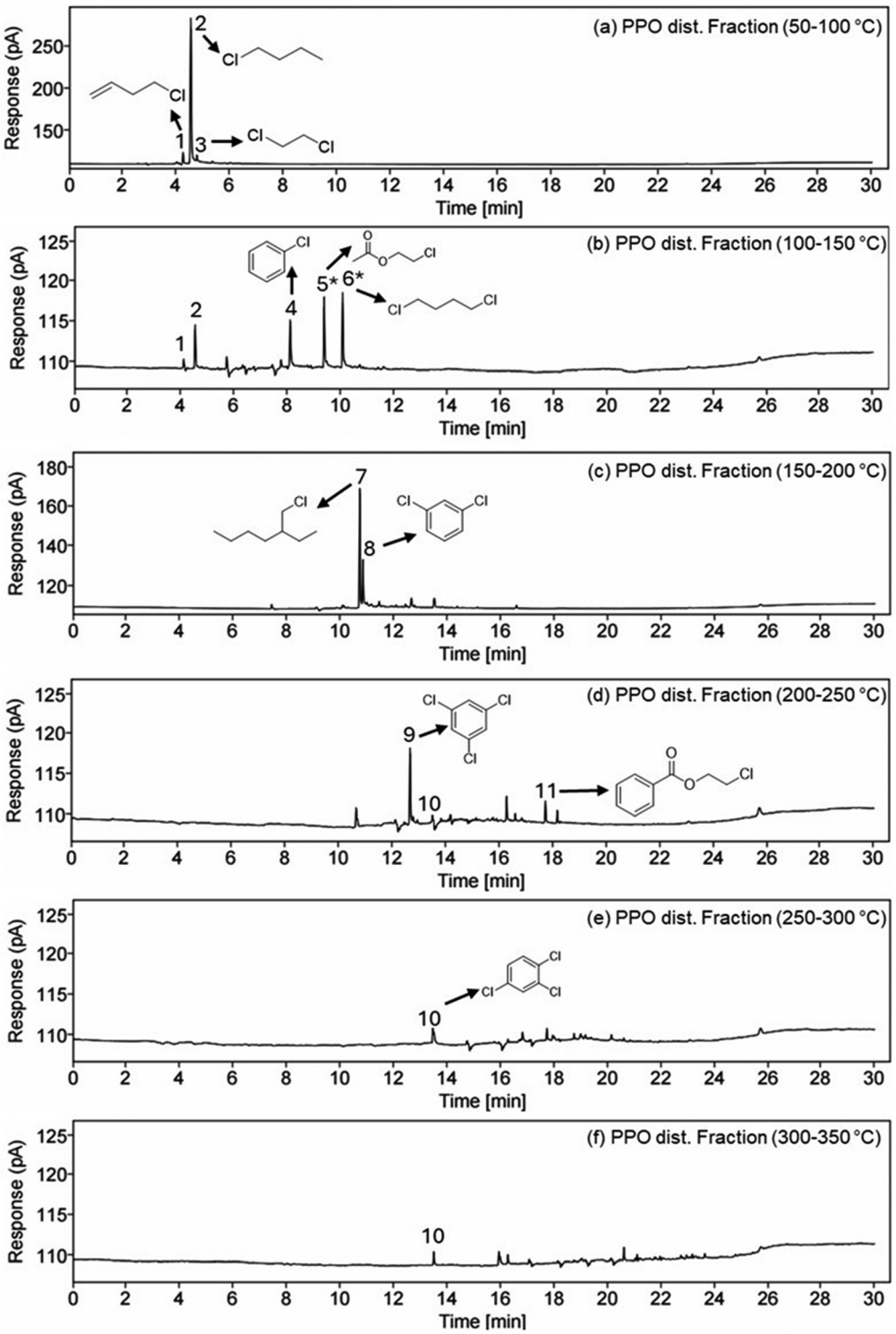

Fig. 5 GC-XSD chromatogram of the PPO distilled fractions collected from different boiling point ranges. Organochlorides identified in the different fractions are shown: (1) 4-chloro-1-butene; (2) 1-chlorobutane; (3) 1,2-dichloroethane; (4) chlorobenzene; (5*) tentatively identified: ethanol, 2-chloro-, acetate; (6*) tentatively identified: 1,4-dichlorobutane; (7) 3-(chloromethyl)heptane; (8) 1,3-dichlorobenzene; (9) 1,3,5-trichlorobenzene; (10) 1,2,4-trichlorobezene; (11) 2-chloroethyl benzoate.

Moreover, 1-chlorobutane, a key compound identified in the lightest PPO fraction, was reported by Souchon *et al.*[21] as the predominant organochloride in two out of three gasoline-range PPO fractions, using a GC-ICP-MS/MS method. One plausible formation pathway for this molecule involves the reaction between chlorine ions and olefins, which are either

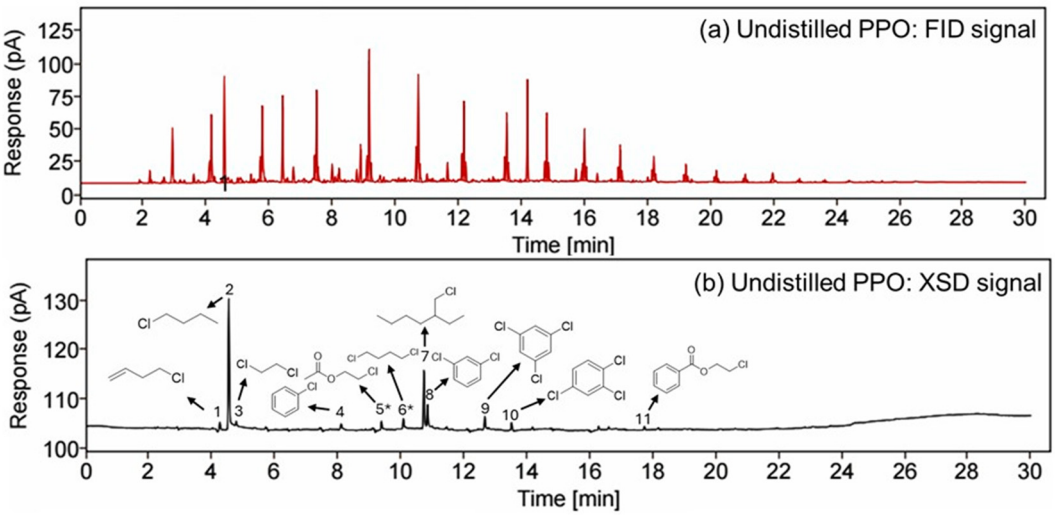

Fig. 6 GC chromatograms of undistilled PPO: (a) FID signal and (b) XSD signal. Organochlorides identified are shown in the GC-XSD chromatogram: (1) 4-chloro-1-butene; (2) 1-chlorobutane; (3) 1,2-dichloroethane; (4) chlorobenzene; (5*) tentatively identified: ethanol, 2-chloro-, acetate; (6*) tentatively identified: 1,4-dichlorobutane; (7) 3-(chloromethyl)heptane; (8) 1,3-dichlorobenzene; (9) 1,3,5 trichlorobenzene; (10) 1,2,4-trichlorobezene; (11) 2-chloroethyl benzoate.

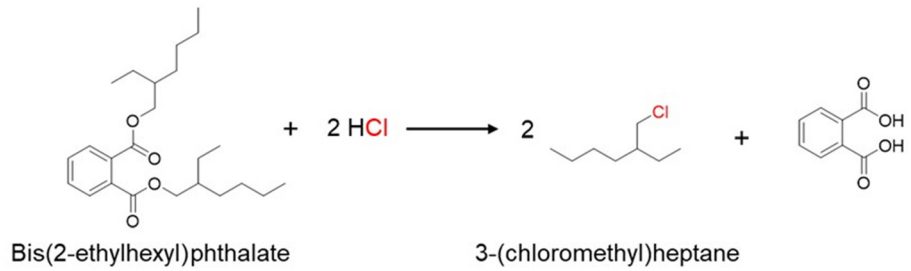

Fig. 7 Proposed reaction pathway for the formation of 3-(chloromethyl)heptane during the pyrolysis of plastic waste.

present in the feedstock or generated during pyrolysis. However, to the best of our knowledge, no specific reaction pathway has yet been proposed for the formation of 1-chlorobutane during the pyrolysis of real plastic waste.

Interestingly, the only chloroester detected in the present study was 2-chloroethyl benzoate, in contrast to our previous work,[23] where several chloroesters were identified. Another notable difference lies in the total chlorine content: in this study, the undistilled PPO contained 67 mg L^{-1} of chlorine, whereas in our previous study, the chlorine content reached 760 mg L^{-1}, both measured using the same analytical method. A recent patent reported that a PPO derived from mixed plastic waste containing PVC had a chlorine content of 40 ppm, while a PPO produced from a feedstock containing both PVC and polyethylene terephthalate (PET) exhibited a significantly higher chlorine level of 700 ppm.[31] This suggests that fragments of polyester might act as a trap for Cl as more Cl compounds can be formed in the process *via* secondary reactions. Several studies have shown that the co-pyrolysis of PET and PVC can lead to the formation of chloroesters, similar to those observed in our earlier work.[15,24,32,33] These findings suggest that the PET content in the mixed plastic waste used in the present study was likely very low, which may have significantly contributed to the reduced formation of organochlorides in the resulting pyrolysis oil. However, this hypothesis should be confirmed in experiments where the waste plastic feed composition is known in more detail.

4. Current gaps and future perspectives

Although the formation of chloroesters has been extensively discussed in the literature, the formation of other organochlorides, such as the linear compounds observed in this study, has been rarely addressed. This knowledge gap presents a valuable opportunity for future research, particularly given that these compounds appear to significantly contribute to the total chlorine content in some PPOs.

In this context, pyrolysis GC analysis (Py-GC)[34,35] of virgin polymers and plastic additives, along with thermogravimetric analysis (TGA),[36] is becoming increasingly relevant, especially

when coupled with selective detectors such as the XSD for organochloride speciation, in combination with MS for molecular identification. Additionally, pyrolysis coupled with comprehensive analytical systems has also been employed to facilitate compound identification.[37] In this regard, evaluating the performance of an XSD detector within such hyphenated systems could also be interesting. These analytical capabilities can greatly enhance the understanding of organochloride formation, which may support the development of strategies to either minimize their formation or improve their removal from PPOs.

Lastly, while several studies have focused on reducing organochloride formation by optimizing pyrolysis conditions, such as using *in situ* absorbents,[38] catalysts[14] or solvents,[39] only a limited number have explored the post-pyrolysis dechlorination of PPOs using adsorbents.[40,41] Detailed speciation of organochlorides and other contaminants in PPOs can be helpful for the design of more selective and efficient adsorbents and help assess their performance and saturation behavior.

5. Conclusions

In this study, a GC coupled with a halogen selective detector (GC-XSD) was evaluated for the identification of organochlorides in hydrocarbon matrices. Key parameters such as detector selectivity, reactor temperature, and response factors for various Cl standards were assessed. Additionally, retention time correlation enabled the use of a GC × GC-HR-TOFMS system for compound identification. Both analytical methods were applied to the distilled fractions of a plastic pyrolysis oil (PPO).

During the analysis of different hydrocarbon matrices, the XSD detector demonstrated high selectivity toward organochlorides. Increased reactor temperatures led to enhanced sensitivity, although this may impact detector lifetime. This parameter can be optimized based on the total chlorine content of the samples. Furthermore, analysis of multiple Cl standards revealed response factor variations across different functional groups, underscoring the importance of selecting appropriate standards for accurate quantification.

The distilled PPO fractions were analyzed using C-IC, GC-XSD and GC × GC-HR-TOFMS. The first (boiling point range: 50–100 °C) and third (boiling point range: 150–200 °C) fractions exhibited the highest chlorine concentrations. 1-Chlorobutane was the most abundant organochloride in the first fraction, while 3-(chloromethyl)heptane, possibly formed *via* reactions between plasticizers and chlorine ions, and 1,3-dichlorobenzene was identified in the third. Other compounds, such as 1,2-dichloroethane, chlorobenzene, and 2-chloroethyl benzoate, were detected at lower concentrations.

The GC-XSD method proved to be a robust and selective tool for routine analysis of PPOs that could be employed in quality control laboratories to speciate and quantify organochlorides in (hydrotreated) PPOs, especially when used alongside total chlorine measurements. While GC × GC-HR-TOFMS is more suited for research and development environments, its combination with GC-XSD offers strong capabilities for identifying unknown species. These analytical tools can deepen the understanding of organochloride formation, thereby supporting the development of strategies to either reduce their formation or enhance their removal from PPOs.

Future work could explore the use of Py-GC(×GC) coupled with XSD and (TOF)MS to gain deeper insights into the formation of organochlorides during pyrolysis, particularly those less frequently reported in the literature, such as linear chlorinated hydrocarbons (*e.g.*, 1-chlorobutane and 1,2-dichloroethane). Additionally, the assessment of other selective detectors such as the AED and the ELCD, as well as hyphenated systems like GC-ICP-MS/MS, and their comparison with the XSD in terms of selectivity, sensitivity, and maintenance, could provide valuable insights for further method developments. Finally, evaluating various adsorbents for selective removal of organochlorides from PPOs and understanding their saturation behavior is crucial for improving process feasibility and enabling integration into existing industrial plants.

Conflicts of interest

There are no conflitcs to declare.

Data availability

The data supporting this article have been included as part of the supplementary information (SI). Supplementary information is available. See DOI: https://doi.org/10.1039/d5an00852b.

Acknowledgements

The authors acknowledge Da Vinci Laboratory Solutions for providing an XSD for demonstration and evaluation over a few months.

References

1 R. Geyer, in *Plastic Waste and Recycling: Environmental Impact, Societal Issues, Prevention, and Solutions*, ed. T. M. Letcher, Academic Press, 1st edn, 2020, ch. 2, pp. 13–32.
2 K. Ragaert, L. Delva and K. V. Geem, *Waste Manage.*, 2017, **69**, 24–58.
3 S. H. Chang, *Sci. Total Environ.*, 2023, **877**, 162719.
4 M. Kusenberg, S. D. Langhe, B. Parvizi, A. J. Abdulrahman, R. J. Varghese, S. U. Aravindakshan, A. Kurkijärvi, A. M. Gandarillas, J. Jamieson, S. D. Meester and K. M. V. Geem, *J. Anal. Appl. Pyrolysis*, 2024, **181**, 106571.

5 C. Mase, J. F. Maillard, B. Paupy, M. Hubert-Roux, C. Afonso and P. Giusti, *ACS Omega*, 2022, **7**, 19428–19436.
6 Y. Ureel, M. L. Chacón-Patiño, M. Kusenberg, R. P. Rodgers, M. K. Sabbe and K. M. V. Geem, *Energy Fuels*, 2024, **38**, 11148–11160.
7 Y. Ureel, M. L. Chacón-Patiño, M. Kusenberg, A. Ginzburg, R. P. Rodgers, M. K. Sabbe and K. M. V. Geem, *Energy Fuels*, 2025, **39**, 1283–1295.
8 M. N. Dunkle, P. Pijcke, W. L. Winniford, M. Ruitenbeek and G. Bellos, *J. Chromatogr. A*, 2021, **1637**, 461837.
9 C. Mase, J. F. Maillard, B. Paupy, M. Farenc, C. Adam, M. Hubert-Roux, C. Afonso and P. Giusti, *Energy Fuels*, 2021, **35**, 14828–14837.
10 H. C. Genuino, M. P. Ruiz, H. J. Heeres and S. R. A. Kersten, *Fuel Process. Technol.*, 2022, **233**, 107304.
11 L. Galan-Sanchez, C. Dittrich, A. van Zijl, T. Housmans, M. Soliman and F. Kuijpers, *Industrial Arene Chemistry: Markets, Technologies, Sustainable Processes and Cases Studies of Aromatic Commodities*, 2023, pp. 2143–2162.
12 M. Kusenberg, A. Eschenbacher, M. R. Djokic, A. Zayoud, K. Ragaert, S. D. Meester and K. M. V. Geem, *Waste Manage.*, 2022, **138**, 83–115.
13 M. Kusenberg, A. Eschenbacher, L. Delva, S. D. Meester, E. Delikonstantis, G. D. Stefanidis, K. Ragaert and K. M. V. Geem, *Fuel Process. Technol.*, 2022, **238**, 107474.
14 Y. Hu, M. Li, N. Zhou, H. Yuan, Q. Guo, L. Jiao and Z. Ma, *Sci. Total Environ.*, 2024, **908**, 168344.
15 P. Gao, Z. Hu, Y. Sheng, W. Pan, L. Ding, L. Tang, X. Chen and F. Wang, *Sci. Total Environ.*, 2024, **912**, 169572.
16 S. Mitra, S. Sulakhe, B. Shown, S. Mandal and A. K. Das, *ChemBioEng Rev.*, 2022, **9**, 319–332.
17 R. Ma, J. Zhu, B. Wu, J. Hu and X. Li, *Energy Fuels*, 2017, **31**, 374–378.
18 B. Wu, Y. Li, X. Li and J. Zhu, *Energy Fuels*, 2015, **29**, 1391–1396.
19 Q. Hao, Z. Yang, B. Wu, J. Zhu, Z. Li, J. Liu and L. Ma, *J. Anal. Appl. Pyrolysis*, 2022, **168**, 105789.
20 O. V. Klimov, K. A. Nadeina, O. V. Potapenko, Yu. V. Vatutina, A. V. Saiko, V. A. Koveza, P. P. Mukhacheva, V. S. Krestyaninova, A. S. Yurtaeva, T. S. Bogomolova, A. A. Salomatina, E. Yu. Gerasimov, I. P. Prosvirin and A. S. Noskov, *Fuel*, 2023, **349**, 128651.
21 V. Souchon, M. Maleval, F. Chainet and C.-P. Lienemann, *J. Anal. At. Spectrom.*, 2023, **38**, 1634–1642.
22 J. Nelson, H. Hopfer, F. Silva, S. Wilbur, J. Chen, K. S. Ozawa and P. L. Wylie, *J. Agric. Food Chem.*, 2015, **63**, 4478–4483.
23 A. Jean, B. C. Magalhaes, P. Pijcke, N. Verhoosel, T. Sanliturk, Y. Ureel, M. Kusenberg, M. Ruitenbeek, G. Bellos, K. M. V. Geem and M. N. Dunkle, *Anal. Chem.*, 2025, **97**, 10680–10690.
24 M. Liu, W. Wang, Q. Zhang, Z. Liu, Y. Li, M. Wu and D. Zhang, *Energy Fuels*, 2023, **37**, 9359–9367.
25 M. S. Klee, in *Gas Chromatography*, ed. C. F. Poole, Elsevier, 1st edn, 2012, pp. 307–347.
26 W. Zhuang, B. McKague, D. Reeve and J. Carey, *J. Chromatogr. A*, 2003, **994**, 137–157.
27 A. Giri, H. Yan, O. Emamjomeh, F. Cuoq, G. Kwakkenbos, A. van Zijl and K. Wong, *Energy Fuels*, 2024, **38**, 8649–8660.
28 W. Zhuang, A. B. McKague, D. W. Reeve and J. H. Carey, *Instrum. Sci. Technol.*, 2005, **33**, 481–507.
29 B. da CostaMagalhães, P. Pijcke, N. Verhoosel, R. Bassie, P. Janssen, C. Benedetti, M. Ruitenbeek, G. Bellos and M. N. Dunkle, *J. Sep. Sci.*, 2025, **48**, e70272.
30 M. Kusenberg, G. C. Faussone, H. D. Thi, M. Roosen, M. Grilc, A. Eschenbacher, S. D. Meester and K. M. V. Geem, *Sci. Total Environ.*, 2022, **838**, 156092.
31 M. Javeed, A. Stanislaus, A. A. Hakeem, G. Koripelly, R. Narayanaswamy and K. K. Ramamurthy, *US Pat*, US10829696B2, 2020.
32 B. Li, X. Wang, Z. Xia, W. Zhou, Y. Wu and G. Zhu, *J. Anal. Appl. Pyrolysis*, 2023, **169**, 105816.
33 I. Coralli, V. Giorgi, I. Vassura, A. G. Rombolà and D. Fabbri, *J. Anal. Appl. Pyrolysis*, 2022, **161**, 105377.
34 R. J. de Korte, M. N. Dunkle, R. van Belzen, A. Battistella and G. Bellos, *Fuel Process. Technol.*, 2025, **267**, 108148.
35 R. Khan, B. A. Perez and H. E. Toraman, *J. Chromatogr. A*, 2024, **1732**, 465243.
36 J. Pan, H. Jiang, T. Qing, J. Zhang and K. Tian, *Chemosphere*, 2021, **284**, 131348.
37 B. A. Perez, J. V. J. Krishna and H. E. Toraman, *J. Chromatogr. A*, 2025, **1739**, 465510.
38 E. Selvam, Z. O. G. Schyns, J. A. Sun, P. A. Kots, Y. Kwak, L. T. J. Korley, R. F. Lobo and D. G. Vlachos, *J. Am. Chem. Soc.*, 2025, **147**, 11227–11238.
39 B. Feng, Y. Jing, X. Liu, Y. Guo and Y. Wang, *Appl. Catal., B*, 2023, **331**, 122671.
40 Q. Sun, B. Huang, L. Bing, D. Han, G. Wang and F. Wang, *Catal. Lett.*, 2025, **155**, 184.
41 A. Romero, I. Moreno, L. Escudero, R. Yuste, P. Pizarro, J. M. Moreno and D. P. Serrano, *J. Environ. Chem. Eng.*, 2024, **12**, 112638.